

HOSTED BY



ELSEVIER

Contents lists available at ScienceDirect

Saudi Journal of Biological Sciences

journal homepage: www.sciencedirect.comالجمعية السعودية لعلم الحياة
SAUDI BIOLOGICAL SOCIETY

Original article

Examining the varied concentrations of *Mentha spicata* and *Ocimum basilicum* affect the synthesis of AgNPs that restrict the development of bacteria

Motahher A. Qaeed

Department of Physical Science, Faculty of Science, University of Jeddah, Jeddah, Saudi Arabia



ARTICLE INFO

Keywords:

AgNPs
Ocimum basilicum
Mentha spicata
Escherichia Coli
Green synthesis and XRD

ABSTRACT

This work examined the effects of varied concentrations of *Ocimum basilicum* and *Mentha spicata* aqueous extracts in order to determine the concentration that has the strongest antibacterial impact through the green synthesis technique of silver nanoparticles (AgNPs). In order to synthesize AgNPs using the reduction method, different quantities of reducing and stabilizing agents: (a) 0.75 mM *Ocimum basilicum* and 0.25 mM *Mentha spicata*; (b) 0.5 *Mentha spicata* and 0.5 mM *Ocimum basilicum*; and (c) 0.25 mM *Ocimum basilicum* and 0.75 mM *Mentha spicata* were utilized. X-ray Diffraction (XRD), and UV-vis spectra were used to analyze AgNPs' crystal structure and shape. The antibacterial potency of *E. coli* ATCC 35218 was investigated utilizing AgNPs employing the well diffusion, MBC, MIC, and the time-kill curve. *Ocimum basilicum* water solution's dark yellow hue denotes the completion of the AgNPs' synthesis. As the aqueous *Ocimum basilicum* solution concentration increases between 0.25 and 0.75 mM, the AgNPs' UV spectra show a gradually increasing absorption. This, in turn, caused the nanoparticle size to alter from 73.57 to 89.05 nm and the wavelength to change from 468 to 474 nm. The experiments also revealed that the nanoparticles had a significantly antibacterial activity against *E. coli*, of the sample prepared with 1 mM *Ocimum basilicum*. Based on the synthesis of AgNPs, it has been shown that an aqueous extract of *Ocimum basilicum* outperforms *Mentha spicata* as a powerful reducing agent and stabilizing agent for the production AgNPs in various sizes. This is true regardless of the solvent content.

1. Introduction

With the advent of nanotechnology, the study with dimensions less than 100 nm of the particle structures has become a focus of numerous scientific projects (Sathishkumar et al., 2012, Mohanta et al., 2017). Owing to their huge surface area to the volume ratio, metallic NPs can be used in many different industries such as biomedicine, optoelectronics, and catalytic processes (Baruah et al., 2019). Recent developments have taken advantage of the unique characteristics of Au, Ag, Pd, and Pt nanometals, including their high stability and conductivity (Zhang et al., 2019). The green synthesis process is popular because it is non-toxic, environmentally friendly, inexpensive (as it does not require any additional reagents), and highly efficient (de Marco et al., 2019, Falcone and Hiete, 2019). These remarkable qualities account for the rising volume of herbal extracts which are utilized to create nanoparticles (Gamboa et al., 2019, Vaid et al., 2020). AgNPs have gained tremendous relevance in recent years due to (1) their photolytically efficiency compared to organic dyes (Samuel et al., 2020), (2) their significant contributions to

the medical field's fight against cancer (Ratan et al., 2020), and (3) their anti-bacterial and antioxidant qualities (Mohanta et al., 2017, Pugazhendhi et al., 2018). AgNPs are made using a range of biological precursors, including plant byproducts, various plant components, and algae (Samuel et al., 2020). Through surface-nanoparticle contact and subsequent capping to prevent the AgNPs generated from aggregating, the leaf aqueous extract contributes significantly to the stability of AgNPs. Numerous plant extracts are utilized for this purpose, including *Bauhinia purpurea* (Chinnappan et al., 2018), *Avicennia marina* (Abdi et al., 2018), *Azadirachaindica* (Mankad et al., 2020), *Limoniaacidissima* (Patil et al., 2012), *Indigofera tinctoria* (Vijayan et al., 2018), *Zingiber-officinale* (Mathew et al., 2018), *Prosopis juliflora* (Arya et al., 2018), *Lagerstroemia speciosa* (Basumatary et al., 2018), *Mentha spicata* (Qaeed et al., 2023b), and *Ocimum basilicum* (Qaeed et al., 2023a).

E-mail address: maqayid@uj.edu.sa.<https://doi.org/10.1016/j.sjbs.2023.103899>

Received 5 November 2023; Received in revised form 3 December 2023; Accepted 8 December 2023

Available online 10 December 2023

1319-562X/© 2023 The Author(s). Published by Elsevier B.V. on behalf of King Saud University. This is an open access article under the CC BY-NC-ND license (<http://creativecommons.org/licenses/by-nc-nd/4.0/>).

2. Methodology

2.1. Materials

Filter papers, silver nitrate, distilled water, *Mentha spicata*, *Ocimum basilicum*, and glass substrates are the materials used in this study.

2.2. The process of making the plant extract

First, the *Mentha spicata* and *Ocimum basilicum* leaves were gathered, washed, dried, and they were powdered up after being finely ground. Next, 10 g of powdered plant material were combined with 100 ml of distilled water. Next, they were swirled for an hour at room temperature in a glass flask using a magnetic stirrer. Then, paper filters were used to filter the aqueous extract of mint plant. This was followed by drying the extract using a dryer. The following, 100 ml of distilled water were added to 1 g of the dry extract. Where it was well-blended for 15 min to create an initial stock solution with a 10,000 ppm concentration. The preparation of additional concentrations from this solution was done.

2.3. Silver nitrate solution preparation

involved taking 0.179 g of silver nitrate and combining it with 100 g of distilled water. As a result, 1 mM is the concentration obtained. 100 ml of distilled water which was combined with 1 ml of AgNO_3 until the solution fully dissolved. Then, 5 ml of silver nitrate was combined with 1 ml of plant extract. We had to wait until the mixture turns liquid, which is the point of the creation of Ag NPs before adding the mixture to the plant extract.

2.4 Glass substrates had to be prepared by cutting them into lengths of $(2.5 \times 2.5) \text{ cm}^2$, Using distilled water (DW) to wash them, and after which 15 min in an ultrasonic machine. After that, the substrates were cleaned of any surface contaminants with 99 % pure acetone solutions before being exposed to the ultrasonic machine once more for ten

minutes.

2.5 Drop Casting: When the solution was ready to precipitate on the substrate, it was homogeneously mixed in an ultrasonic device before being poured into a dropper. After that, after that, the solution was dried by distillation onto a heated substrate at 50°C , as illustrated in Fig. 1.

3. Microbial studies

3.1. Strains of bacteria and it's Growth

Escherichia coli ATCC 35218, the bioreporter utilized in this investigation, was purchased from Thermo Scientific™ Culti-Loops™. The bacteria were grown in NB broth with 24 % glycerol overnight, and then kept at 75°C . The bacteria were kept until they were required. After being removed from the glycerol stock, the bacteria were grown in Nutrient-Broth (NB) medium before being applied. The experiment employed 10 ml of NB broth per day to transfer culture to a glass tube, where it was then cultivated on a MacConkey agar plate.

3.2. In vitro susceptibility test

3.2.1. Agar well diffusion assay

At a concentration of 10^7 CFU/mL, *Escherichia coli* was employed to inoculate Mueller Hinton Agar Media (MHA). Each culture plate has six 6 mm holes bored onto it using a cork borer. Different concentrations of sterilized distilled water (SDW) were added to 100 L of the samples as a negative control. At 37°C , the plates were incubated for 24 h. The mean and standard deviation (SD) of trials conducted in triplicate served as the zone of inhibition measurements (Al-Masaudi and Al-Maaqar, 2020).

3.2.2. Estimation of minimum inhibitory concentrations (MIC) of *Ocimum basilicum* and *Mentha spicata*

In most cases, 96 well microtiter plates are used in micro-broth dilution tests to determine minimum inhibitory concentrations (MICs).

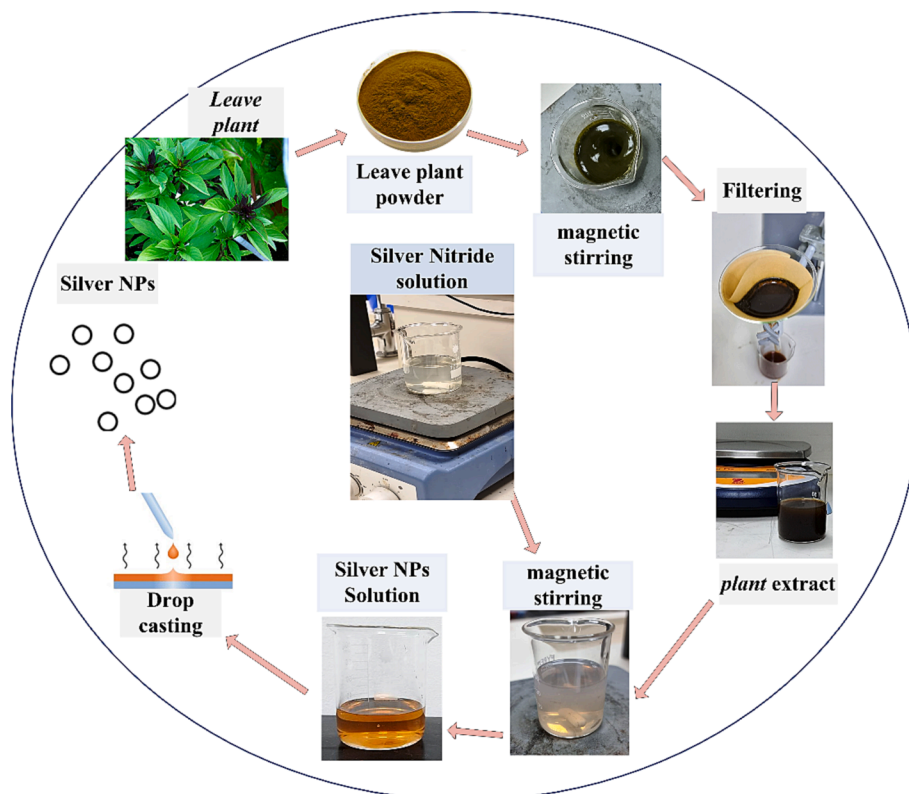


Fig. 1. Methodology graphical shape of synthesis AgNPs.

So, in order to determine the MICs of samples against bacteria, MICs were handled using the micro-diluted broth technique as defined by NCCLS (Sedighinia et al., 2012). 24 h were spent on incubating the sample at 37 °C. Each well received 10 μ L of the Resazurin sodium salt dye (R7017 Sigma-Aldrich) upon incubation (Elshikh et al., 2016). Column 12 just confirms that there was no contamination of the plate during dish preparation. It acts as a negative control and contains media. *Ocimum basilicum* and *Mentha spicata* were serially diluted with media in column 2–11, while the solely-medium-cultured strain in column 1 is a positive control.

3.2.3. Estimation of minimal bactericidal concentrations (MBC) *Ocimum basilicum* and *Mentha spicata*

The lowest quantity of the samples treated with NPs at which were killed the injected bacteria is known as the minimal bactericidal concentration (MBC). They re-inoculated 10 L of media from the MIC's microplate contents on nutrient agar plates and then incubated them at 37 °C for 24 h without any bacterial growth. The first well was determined to be growth-negative and reported as the MBC when the colony counts were < 5 (Elshikh et al., 2016).

3.2.4. Time-kill kinetics

Determination of time-kill kinetics for a bacterial strain, the highest MIC concentration for the samples and Augmentin were measured. At 37 °C, cultures were cultured aerobically, and AgNPs and Augmentin solutions were introduced to perform antibiotic concentrations. Following the addition of AgNPs and an antibiotic solution to the well at the time periods of 0, 2, 4, 6, 8, 10, 12 and 24 h, samples of the cultures were aseptically removed. On blood agar plates, 0.001 μ L of sterilized loops were incubated for 24 h at 37 °C. Using a plate counter, bacteria colonies were counted (Monica, 2006).

4. Results

4.1. Uv-vis light of AgNPs synthesized used *Mentha spicata* and *Ocimum basilicum*

The spectrum of AgNPs produced at various UV-absorbing ratios of *Mentha spicata* and *Ocimum basilicum* from a to c ((a) 0.75 mM *Ocimum basilicum* & 0.25 mM *Mentha spicata* (b) 0.5 mM *Mentha spicata* & 0.5 mM *Ocimum basilicum* and (c) 0.25 mM *Ocimum basilicum* & 0.75 mM *Mentha spicata*) were recorded and drawn in Fig. 2. as the color gradient of AgNPs shown in Fig. 3.

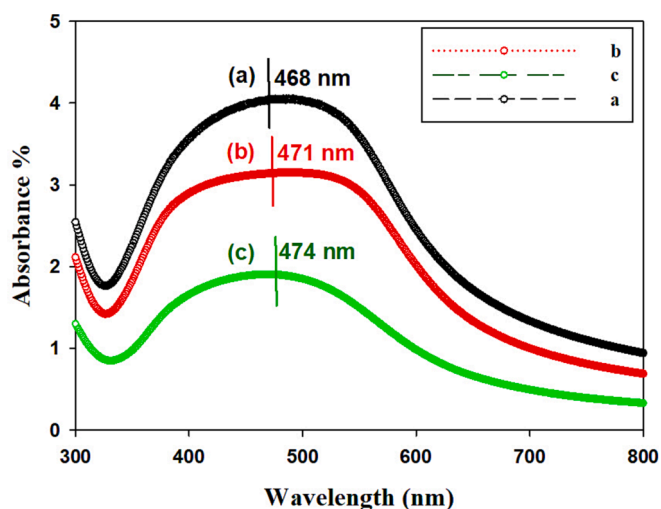


Fig. 2. UV-Spectroscopy of AgNPs synthesized with (a) 0.75 mM *Ocimum basilicum* & 0.25 mM *Mentha spicata* (b) 0.5 mM *Mentha spicata* & 0.5 mM *Ocimum basilicum* and (c) 0.25 mM *Ocimum basilicum* & 0.75 mM *Mentha spicata*.

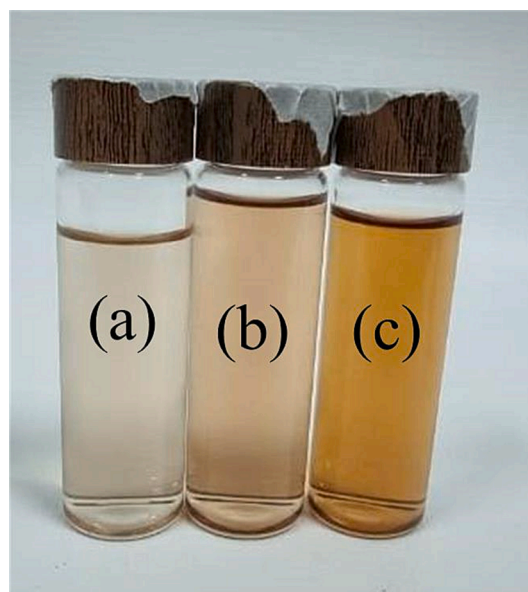


Fig. 3. Color gradient of AgNPs synthesized with (a) 0.75 mM *Ocimum basilicum* & 0.25 mM *Mentha spicata* (b) 0.5 mM *Mentha spicata* & 0.5 mM *Ocimum basilicum* and (c) 0.25 mM *Ocimum basilicum* & 0.75 mM *Mentha spicata*.

4.2. XRD Diffraction of AgNPs synthesized with *Ocimum basilicum* and *Mentha spicata*

This section describes the production of AgNPs using various quantities of water solutions of *Ocimum basilicum* and *Mentha spicata*: (a) 0.75 mM *Ocimum basilicum* & 0.25 mM *Mentha spicata* (b) 0.5 mM *Mentha spicata* & 0.5 mM *Ocimum basilicum* and (c) 0.25 mM *Ocimum basilicum* & 0.75 mM *Mentha spicata* as a bio-solvent. The result displayed in Fig. 4 and Table 1.

4.3. FESEM image of AgNPs synthesized with 0.75 mM of *Ocimum basilicum* and 0.25 mM of *Mentha spicata*

This investigation describe the shape and size of AgNPs for the best sample synthesized with 0.75 mM of *Ocimum basilicum* and 0.25 mM of *Mentha spicata*.

4.4. Antibacterial test using agar diffusion assay

The goal of this study was to compare the antibacterial properties of two different solvents used to create AgNPs *Mentha spicata* and *Ocimum basilicum* with varying ratios (1) 1 mM *Mentha spicata*, (2) 0.75 mM *Mentha spicata* & 0.25 mM *Ocimum basilicum*, (3) 0.5 mM *Mentha spicata* & 0.5 mM *Ocimum basilicum*, (4) 0.75 mM *Ocimum basilicum* & 0.25 mM *Mentha spicata* and (5) 1 mM *Ocimum basilicum*. The findings of the well diffusion investigation shown in Fig. 5, the MIC and MBC of the samples, and the antibacterial activity of the five samples were assessed against Gram-negative bacterium, *E. coli* ATCC 35218.

4.5. Antibacterial investigation utilizing MIC and MBC

However, a more thorough examination was needed to determine the antibacterial activation of the samples utilizing the MIC value. The well diffusion test was reported as a preliminary investigation in screening an antimicrobial agent's antibacterial activity. The MIC was established as the lowest concentration of antibacterial agent which is necessary to prevent bacterial growth by serial dilution. As showed in Fig. 7,

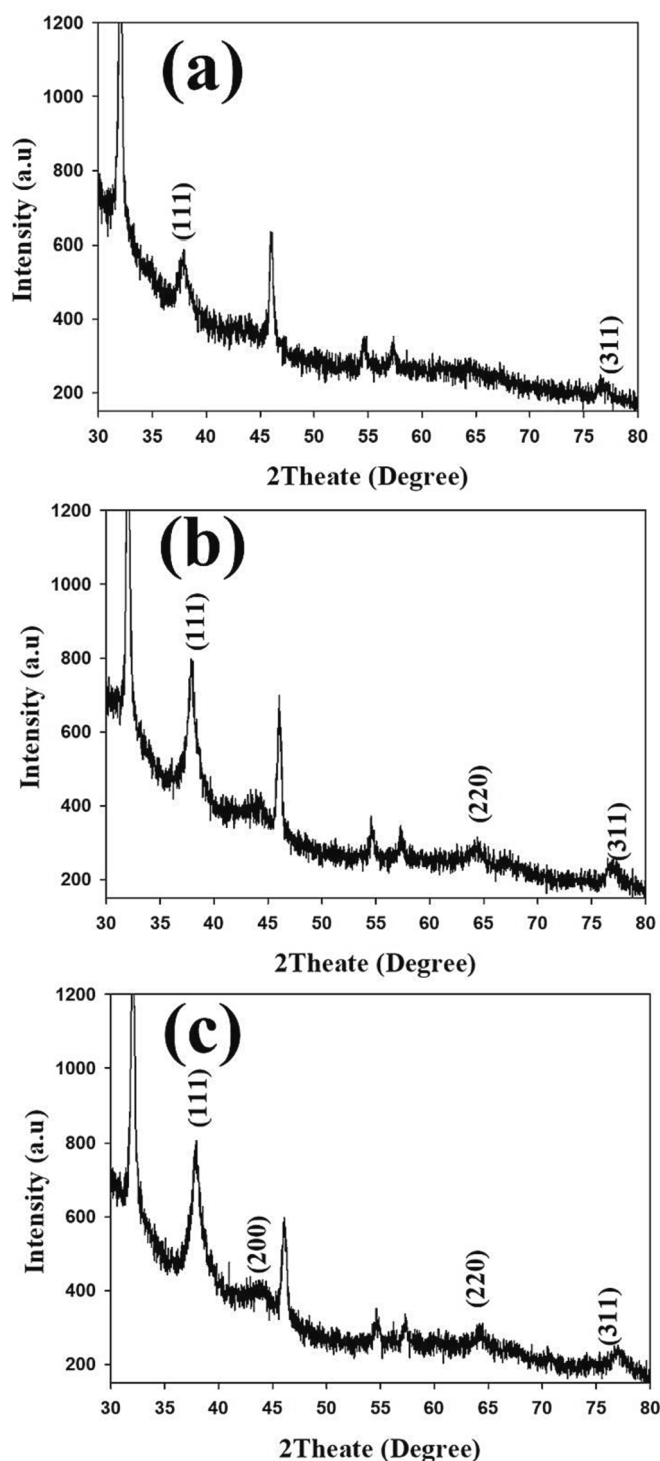


Fig. 4. XRD measurement of AgNPs synthesized with (a) 0.75 mM *Ocimum basilicum* & 0.25 mM *Mentha spicata* (b) 0.5 mM *Mentha spicata* & 0.5 mM *Ocimum basilicum* and (c) 0.25 mM *Ocimum basilicum* & 0.75 mM *Mentha spicata*.

4.6. Time-kill kinetics

The sample's time-killing curves, which were created using 1 mm of *Ocimum basilicum* extract, showed less efficacy than Augmentin (Fig. 8).

Table 1

XRD measurement of AgNPs synthesized with (a) 0.75 mM *Ocimum basilicum* & 0.25 mM *Mentha spicata* (b) 0.5 mM *Mentha spicata* & 0.5 mM *Ocimum basilicum* and (c) 0.25 mM *Ocimum basilicum* & 0.75 mM *Mentha spicata*.

Sample	2theta (deg)	d(A°)	Phase name	FWHM (deg)	Nano particle Size (A°)
a	37.814	2.37717	111	1.1921	73.57
b	37.8382	2.3757	111	0.9849	89.05
c	37.8256	2.37646	111	1.1574	75.78

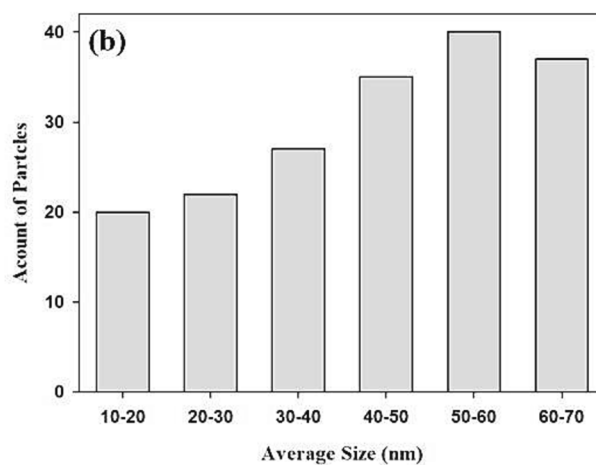
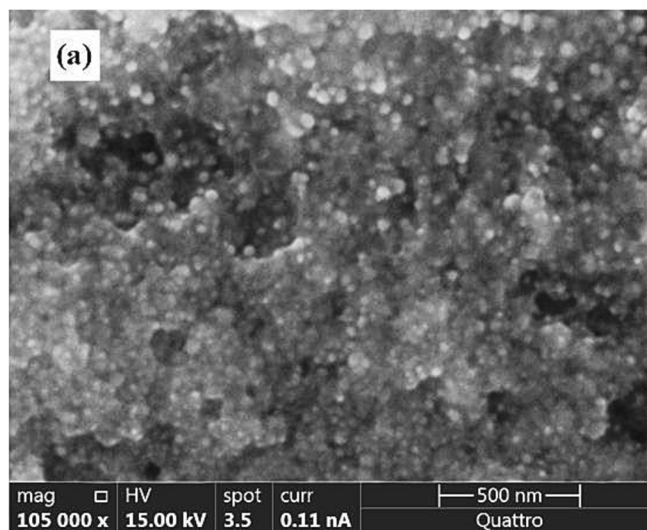


Fig. 5. (a) FESEM image of AgNPs synthesized with synthesized with 0.75 mM of *Ocimum basilicum* and 0.25 mM of *Mentha spicata* (b) AgNPs sizes distribution.

5. Discussion

5.1. Uv-vis light of AgNPs synthesized used *Mentha spicata* and *Ocimum basilicum*

The spectrum of AgNPs produced at various UV-absorbing ratios of *Mentha spicata* and *Ocimum basilicum* from a to c ((a) 0.75 mM *Ocimum basilicum* & 0.25 mM *Mentha spicata* (b) 0.5 mM *Mentha spicata* & 0.5 mM *Ocimum basilicum* and (c) 0.25 mM *Ocimum basilicum* & 0.75 mM *Mentha spicata*) were recorded. The reduction of silver ions, which produced the nanoparticles, is shown by the color shift from colorless to light orange that was seen in the diluted extracts. The bulk substance devoid of a

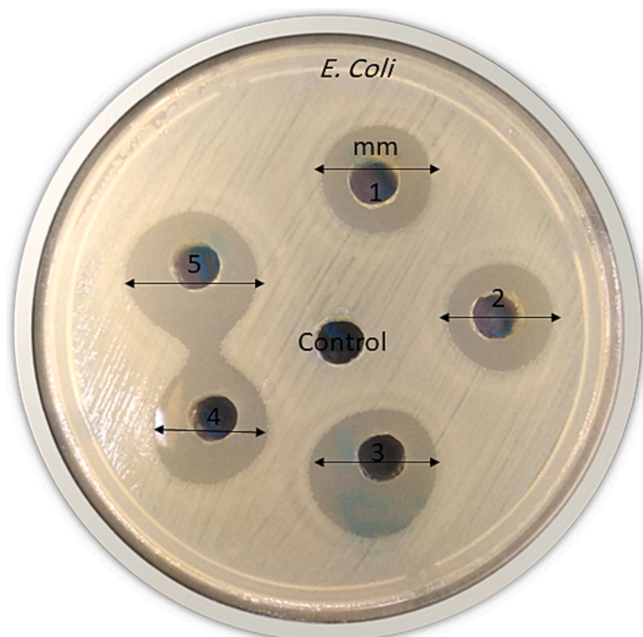


Fig. 6. Inhibition zone (mm) of ((1) 1 *Mentha spicata*, (2) 0.75 *Mentha spicata* & 0.25 *Ocimum basilicum*, (3) 0.5 *Mentha spicata* & 0.5 *Ocimum basilicum*, (4) 0.75 *Ocimum basilicum* & 0.25 *Mentha spicata* and (5) 1 *Ocimum basilicum*) Mm; Control; sterilized distilled water (SDW), by agar Well diffusion method against *Escherichia coli* ATCC 35218.



Fig. 7. Determination of MIC and MBC of ((1) 1 *Mentha spicata*, (2) 0.75 *Mentha spicata* & 0.25 *Ocimum basilicum*, (3) 0.5 *Mentha spicata* & 0.5 *Ocimum basilicum*, (4) 0.75 *Ocimum basilicum* & 0.25 *Mentha spicata* and (5) 1 *Ocimum basilicum*) Mm, C+; cultured strain with media; C-; only media, MIC; Minimum inhibitory concentrations, and MBC; Minimal bactericidal concentrations, against pathogenic bacteria (*Escherichia Coli*) using Resazurin dye.

bandgap, It has a band gap when it gets low-dimensional. The particle size affects this band gap; the smaller the particle size, the larger the band gap. The aqueous solution of particles has distinct hues due to surface plasmon resonance, which is caused by varying band gaps leading to different light absorption. When light strikes silver nanoparticles with free electrons, the absorption band of plasmonic resonance develops due to the reciprocal vibration of the incoming light wave and the electrons. The absorption peaks and silver particles exhibit plasmonic resonance properties, with a steady drop in absorption from 468 to 472 nm. Because the bandwidth decreases as the surface plasmon resonance strength rises, it was found that the FWHM varied for each sample (Zhang et al., 2006). Because a higher concentration of *Ocimum*

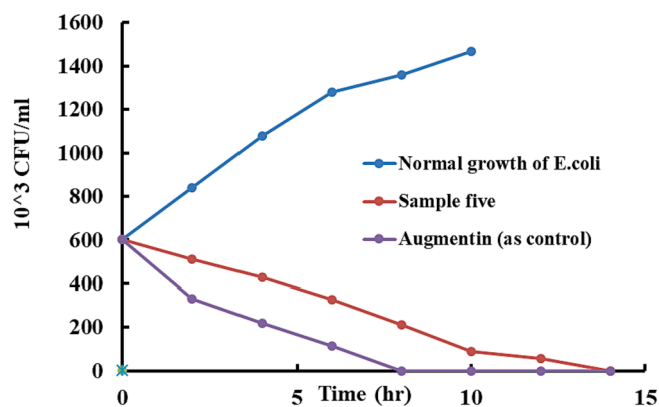


Fig. 8. Time-Killing curve for *Echrechia coli* ATCC 35218 of sample synthesized with 1 mM *Ocimum basilicum* and Augmentin as control.

basilicum extract led to a higher of absorption level, in Fig. 2 the peaks further show the relevance of the ratio of *Ocimum basilicum* leaves to *Mentha spicata* leaves. (Anandalakshmi et al., 2016). From Fig. 2, it can be observed that the peaks are located between 468 and 474 nm, noting that there is a red shift in these peaks toward an increase in wavelength with the increase in particle size brought on by a differ in the solution color of the AgNPs. The rise in the particle size shown in Fig. 3 correlates to findings reported in previous studies (Kelly et al., 2003, Jain et al., 2006). As the concentration of the *Ocimum basilicum* extract rises, *Ocimum basilicum* leaves contain more crucial substances needed for the transformation of Ag + into Ag⁰. This explains the difference between the amounts of *Ocimum basilicum* extract and *Mentha spicata* extract in terms of the change in absorption intensity (Njagi et al., 2011).

5.2. XRD Diffraction of AgNPs synthesized with *Ocimum basilicum* and *Mentha spicata*

This section describes the production of AgNPs using various quantities of water solutions of *Ocimum basilicum* and *Mentha spicata*: (a) 0.75 mM *Ocimum basilicum* & 0.25 mM *Mentha spicata* (b) 0.5 mM *Mentha spicata* & 0.5 mM *Ocimum basilicum* and (c) 0.25 mM *Ocimum basilicum* & 0.75 mM *Mentha spicata* as a bio-solvent. They were investigated using XRD to establish the development of silver nanoparticles and related structural forms. The main peaks of the model are evidently located at 2θ of 37.86, 44.07, 64.22 and 77.17, corresponding to the planes (1 1 1), (200), (2 2 0) and (3 1 1), respectively (Anandalakshmi et al., 2016). This corresponds to (File No.: 89–3722). The fcc structure of AgNPs was discovered through this investigation, and the Scherer equation was used to calculate the particle sizes. By calculating the Bragg reflection width (FWHM) from the measurement findings, each sample's estimated average particle size was determined. They were 73.57, 89.05 and 75.78 for the samples (a) 0.75 mM *Ocimum basilicum* & 0.25 mM *Mentha spicata* (b) 0.5 mM *Mentha spicata* & 0.5 mM *Ocimum basilicum* and (c) 0.25 mM *Ocimum basilicum* & 0.75 mM *Mentha spicata*, respectively, as shown in the Table 1. According to the ratios of basil and micon utilized in the synthesis of nanoparticles, it is clear that each sample has closed particle sizes and that the growth of the particles is polycrystalline. The high peak at level 1.1.1 was produced by the majority of atoms diffracting the x-ray from the same level. This was also noted in a previous study (Ahmad et al., 2010). Additionally, each sample's peak, as shown in Fig. 4, has a larger intensity ratio at peak (1 1 1), compared to the other peaks. This clearly shows that this level's growth was simpler than the others and that it increases in concentration as silver ions build up on it (Ahmad et al., 2010). The two unidentified peaks at angles might have been caused by the presence of compounds in the aqueous leaf solution of *Ocimum basilicum* and *Mentha spicata* (32.25 and 46.21) or the compounds that still attach to the nanoparticles' surfaces (Kumar and Yadav, 2009, Suvith and Philip, 2014). According to Jeeva et al., The

phytochemicals found in leaf extracts, where they are most abundant, show that silver is an important component of biosynthesis, cause the crystalline peaks (32.28, 46.28, 54.83, 67.47, and 76.69) that occurred in the XRD investigation (Jeeva et al., 2014).

5.3. FESEM image of AgNPs synthesized with 0.75 Mm of *Ocimum basilicum* and 0.25 mM of *Mentha spicata*

The AgNPs material synthesized through a 0.75 mM extract of *Ocimum basilicum* was captured in a FESEM image. This demonstrates unequivocally that spherical forms are hints to silver nanoparticles, or AgNPs. The provided picture Fig. 5 (a) illustrates the some holes on the sample surface. The AgNPs size distribution is depicted in image Fig. 5 (b), where the average size is seen to be between 50 and 60 nm, in agreement with the XRD findings.

5.4. Antibacterial test using agar diffusion assay

The goal of this study was to compare the antibacterial properties of two different solvents used to create AgNPs *Mentha spicata* and *Ocimum basilicum* with varying ratios (1) 1 mM *Mentha spicata*, (2) 0.75 mM *Mentha spicata* & 0.25 mM *Ocimum basilicum*, (3) 0.5 mM *Mentha spicata* & 0.5 mM *Ocimum basilicum*, (4) 0.75 mM *Ocimum basilicum* & 0.25 mM *Mentha spicata* and (5) 1 mM *Ocimum basilicum*. The findings of the well diffusion investigation, the MIC and MBC of the samples, and the antibacterial activity of the five samples were assessed against Gram-negative bacterium, *E. coli* ATCC 35218.

The appearance of a clean zone around the well in the well diffusion test indicates that the five samples have antibacterial action, which might stop the growth of the Gram-negative infection. The outcome of this work showed that the obstruction zones against *Escherichia coli* ATCC 35218 range from a minimum of 16.06 mm to a high of 19.05 mm. The compounds' inhibitory effects varied based on the solvent concentrations, as reported in Fig. 6. The sample synthesized with 1 Mm *Ocimum basilicum* had a huge activity (19 ± 0.5 mm zone diameter) against *Escherichia coli*, while the sample produced with 1 mM *Mentha spicata* had a little activity (16 mm) against *Escherichia coli*.

5.5. Antibacterial investigation utilizing MIC and MBC

However, a more thorough examination was needed to determine the antibacterial activation of the samples utilizing the MIC value. The well diffusion test was reported as a preliminary investigation in screening an antimicrobial agent's antibacterial activity. The MIC was established as the lowest concentration of antibacterial agent which is necessary to prevent bacterial growth by serial dilution. As showed in Fig. 7, the samples were diluted threefold, and their MIC values against the pathogenic bacteria were tested. These samples were synthesized using 1 mM *Ocimum basilicum*. MBC is the bacterial inhibitor with the lowest effective bacterial killing concentration. In this work, MBC for *E. coli* diluted two of the sample synthesized with 1 Mm *Ocimum basilicum*, as reflected in Fig. 7. Sample five synthesized with 1 mM *Ocimum basilicum* was more active, compared to the other four samples which were confirmed by the MIC test, and it is considered to be the most sensitive diffusion test, compared to the agar diffusion test.

5.6. Time-kill kinetics

The sample's time-killing curves, which were created using 1 mm of *Ocimum basilicum* extract, showed less efficacy than Augmentin (Fig. 8). Moreover, the values of sample synthesized with 1 mM *Ocimum basilicum* indicated more effect than other samples. These results were obtained according to MIC test. All germs were fully dead after an incubation period of 6 to 12 h. In the current investigation, bacterial density for all strains quickly rose in the absence of antibiotic. The pathogenic bacteria in sample five, which was produced with 1 Mm

Ocimum basilicum, were the first to reduce in quantity while they were still at the MIC. After 12 h of incubation, they died, whereas there was between 12 and 24 h of incubation, no bacterial growth occurred.

6. Conclusion

The green synthesis approach, which uses the aqueous extract of *Ocimum basilicum* and *Mentha spicata* as a reduction and stabilizing agent in various amounts, has proved successful in producing Ag NPs that are less expensive, ecologically friendly, and hazardous. Ag NPs with closed diameters ranging from 73.57 to 89.05 nm were visible in the outcomes. The optimal concentration of 0.75 mM of *Ocimum Basilicum* extract solution, these results in tiny particles, helps break down the biological barrier of bacteria, and kills it. In the visible light, spherical AgNPs have a maximal absorption. AgNPs treated with *Ocimum basilicum* and *Mentha spicata* in various ratios show substantial antibacterial action against *Escherichia coli* ATCC 35218. As a result, *Ocimum Basilicum* may be a more ensuring choice than *Mentha spicata* for generating AgNPs structures that result in a single crystalline rather than *Mentha spicata*'s ability to synthesis a multicrystalline when utilized as a harmful microorganism-targeting antibacterial agent. *Ocimum basilicum* may be used to make useful discoveries in a variety of sectors, including medical technology and antibacterial systems.

Declaration of competing interest

The authors declare that they have no known competing financial interests or personal relationships that could have appeared to influence the work reported in this paper.

Acknowledgments

This work was funded by the University of Jeddah, Jeddah, Saudi Arabia, under grant.

No. (UJ-23-DR-201). Therefore, the authors thank the University of Jeddah for itstechnical and financial support

References

- Abdi, V., Sournejad, I., Yousefzadi, M., Ghasemi, Z., 2018. Mangrove-mediated synthesis of silver nanoparticles using native *avicennia marina* plant extract from southern Iran. *Chem. Eng. Commun.*
- Ahmad, N., Sharma, S., Alam, M.K., Singh, V., Shamsi, S., Mehta, B., Fatma, A., 2010. Rapid synthesis of silver nanoparticles using dried medicinal plant of basil. *Colloids and Surf. B: Biointerfaces*.
- Al-Masaudi, S.B., Al-Maaqar, S.M.S., 2020. Susceptibility of multidrug-resistant enteric pathogenic diarrheal bacteria to Saudi honey. *J. King Abdulaziz Univ.: Sci.*
- Anandalakshmi, K., Venugobal, J., Ramasamy, V., 2016. Characterization of silver nanoparticles by green synthesis method using *pedalium murex* leaf extract and their antibacterial activity. *Appl. Nanosci.*
- Arya, G., Kumari, R.M., Gupta, N., Kumar, A., Chandra, R., Nimesh, S., 2018. Green synthesis of silver nanoparticles using *prosopis juliflora* bark extract: Reaction optimization, antimicrobial and catalytic activities. *Artif. Cells, Nanomed., Biotechnol.*
- Baruah, D., Yadav, R.N.S., Yadav, A., Das, A.M., 2019. *Alpinia nigra* fruits mediated synthesis of silver nanoparticles and their antimicrobial and photocatalytic activities. *J. Photochem. Photobiol. B Biol.*
- Basumatary, K., Daimary, P., Das, S.K., Thapa, M., Singh, M., Mukherjee, A., Kumar, S., 2018. *Lagerstroemia speciosa* fruit-mediated synthesis of silver nanoparticles and its application as filler in agar based nanocomposite films for antimicrobial food packaging. *Food Packag. Shelf Life*.
- Chinnappan, S., Kandasamy, S., Arumugam, S., Seralathan, K.-K., Thangaswamy, S., Muthusamy, G., 2018. Biomimetic synthesis of silver nanoparticles using flower extract of *baubhinia purpurea* and its antibacterial activity against clinical pathogens. *Environ. Sci. Pollut. Res.*
- de Marco, B.A., Rechele, B.S., Tótolí, E.G., Kogawa, A.C., Salgado, H.R.N., 2019. Evolution of green chemistry and its multidimensional impacts: A review. *Saudi Pharmaceut. J.*
- Elshikh, M., Ahmed, S., Funston, S., Dunlop, P., McGaw, M., Marchant, R., Banat, I.M., 2016. Resazurin-based 96-well plate microdilution method for the determination of minimum inhibitory concentration of biosurfactants. *Biotechnol. Lett.*
- Falcone, P.M., Hiete, M., 2019. Exploring green and sustainable chemistry in the context of sustainability transition: The role of visions and policy. *Curr. Opin. Green Sustain. Chem.*

- Gamboa, S.M., Rojas, E., Martínez, V., Vega-Baudrit, J., 2019. Synthesis and characterization of silver nanoparticles and their application as an antibacterial agent. *Int. J. Biosen. Bioelectron.*
- Jain, P.K., Lee, K.S., El-Sayed, I.H., El-Sayed, M.A., 2006. Calculated absorption and scattering properties of gold nanoparticles of different size, shape, and composition: Applications in biological imaging and biomedicine. *J. Phys. Chem. B.*
- Jeeva, K., Thiagarajan, M., Elangovan, V., Geetha, N., Venkatachalam, P., 2014. *Caesalpinia coriaria* leaf extracts mediated biosynthesis of metallic silver nanoparticles and their antibacterial activity against clinically isolated pathogens. *Ind. Crop. Prod.*
- Kelly, K.L., Coronado, E., Zhao, L.L., Schatz, G.C., 2003. The optical properties of metal nanoparticles: The influence of size, shape, and dielectric environment. *ACS Publications.* 107, 668–677.
- Kumar, V., Yadav, S., 2009. Plant-mediated synthesis of silver and gold nanoparticles and their applications. *Chem. Technol. Biotechnol.*
- Mankad, M., Patil, G., Patel, D., Patel, P., Patel, A., 2020. Comparative studies of sunlight mediated green synthesis of silver nanoparticles from *azadirachta indica* leaf extract and its antibacterial effect on *xanthomonas oryzae* pv. *Oryzae*. *Arab. J. Chem.*
- Mathew, S., Prakash, A., Radhakrishnan, E., 2018. Sunlight mediated rapid synthesis of small size range silver nanoparticles using zingiber officinale rhizome extract and its antibacterial activity analysis. *Inorganic and Nano-Metal Chemistry.*
- Mohanta, Y.K., Panda, S.K., Jayabalan, R., Sharma, N., Bastia, A.K., Mohanta, T.K., 2017. Antimicrobial, antioxidant and cytotoxic activity of silver nanoparticles synthesized by leaf extract of *erythrina suberosa* (roxb.). *Front. Mol. Biosci.*
- Monica, C., 2006. *District laboratory practice in tropical countries.* Cambridge University Press, New York.
- Njagi, E.C., Huang, H., Stafford, L., Genuino, H., Galindo, H.M., Collins, J.B., Hoag, G.E., Suib, S.L., 2011. Biosynthesis of iron and silver nanoparticles at room temperature using aqueous sorghum bran extracts. *Langmuir.*
- Patil, R.S., Kokate, M.R., Kolekar, S.S., 2012. Bioinspired synthesis of highly stabilized silver nanoparticles using *ocimum tenuiflorum* leaf extract and their antibacterial activity. *Spectrochimica Acta Part A: Molecular and Biomolecular Spectroscopy.*
- Pugazhendhi, A., Prabakar, D., Jacob, J.M., Karuppusamy, I., Saratale, R.G., 2018. Synthesis and characterization of silver nanoparticles using *gellidium amansii* and its antimicrobial property against various pathogenic bacteria. *Microbial Pathogenesis.*
- M.A. Qaeed A. Hendi A.S. Obaid A.A. Thahe A.M. Osman A. Ismail A. Mindil A.A. Eid F. Aqlan N.M.A. Osman A. Al-Farga S.M. Al-Maaqar Saif, A.e.A., The effect of different aqueous solutions ratios of *ocimum basilicum* utilized in agnps synthesis on the inhibition of bacterial growth *Scientific reports* 2023 10.1038/s41598-023-31221-7.
- Qaeed, M.A., Hendi, A., Thahe, A.A., Al-Maaqar, S.M., Osman, A.M., Ismail, A., Mindil, A., Eid, A.A., Aqlan, F., Al-Nahari, E., 2023b. Effect of different ratios of *mentha spicata* aqueous solution based on a biosolvent on the synthesis of agnps for inhibiting bacteria. *J. Nanomater.*
- Ratan, Z.A., Haidere, M.F., Nurunnabi, M., Shahriar, S.M., Ahammad, A., Shim, Y.Y., Reaney, M.J., Cho, J.Y., 2020. Green chemistry synthesis of silver nanoparticles and their potential anticancer effects. *Cancers.*
- Samuel, M.S., Selvarajan, E., Mathimani, T., Santhanam, N., Phuong, T.N., Brindhadevi, K., Pugazhendhi, A., 2020. Green synthesis of cobalt-oxide nanoparticle using jumbo muscadine (*vitis rotundifolia*): Characterization and photo-catalytic activity of acid blue-74. *J. Photochem. Photobiol. B Biol.*
- Sathishkumar, G., Gobinath, C., Karpagam, K., Hemamalini, V., Premkumar, K., Sivaramakrishnan, S., 2012. Phyto-synthesis of silver nanoscale particles using *morinda citrifolia* l. And its inhibitory activity against human pathogens. *Colloids and Surfaces B: Biointerfaces.*
- Sedighinia, F., Afshar, A.S., Asili, J., Ghazvini, K., 2012. Antibacterial activity of glycyrrhiza glabra against oral pathogens: An in vitro study. *Avicenna journal of phytomedicine.*
- Suvith, V., Philip, D., 2014. Catalytic degradation of methylene blue using biosynthesized gold and silver nanoparticles. *Spectrochimica Acta Part A: Molecular and Biomolecular Spectroscopy.*
- Vaid, P., Raizada, P., Saini, A.K., Saini, R.V., 2020. Biogenic silver, gold and copper nanoparticles-a sustainable green chemistry approach for cancer therapy. *Sustain. Chem. Pharm.*
- Vijayan, R., Joseph, S., Mathew, B., 2018. *Indigofera tinctoria* leaf extract mediated green synthesis of silver and gold nanoparticles and assessment of their anticancer, antimicrobial, antioxidant and catalytic properties. *Artificial cells, nanomedicine, and biotechnology.*
- Zhang, W., Qiao, X., Chen, J., 2006. Synthesis and characterization of silver nanoparticles in aot microemulsion system. *Chem. Phys.*
- Zhang, X., Sun, H., Tan, S., Gao, J., Fu, Y., Liu, Z., 2019. Hydrothermal synthesis of ag nanoparticles on the nanocellulose and their antibacterial study. *Inorg. Chem. Commu.*